

Pattern formation without heating in an evaporative convection experiment

HECTOR MANCINI(*) AND DIEGO MAZA

*Departamento de Física y Matemática Aplicada. Facultad de Ciencias
Universidad de Navarra. 31080 Pamplona, Navarra, Spain.*

PACS. 47.54.+r – Pattern selection; pattern formation.

PACS. 47.20.Dr – Surface-tension-driven instability.

PACS. 47.20.Hw – Morphological instability; phase changes.

Abstract. – We present an evaporation experiment in a single fluid layer reproducing conditions of volatile fluids in nature. When latent heat associated to the evaporation is large enough, the heat flow through the free surface of the layer generates temperature gradients that can destabilize the conductive motionless state giving rise to convective cellular structures without any external heating. Convective cells can be then observed in the transient range of evaporation from an initial depth value to a minimum threshold depth, after which a conductive motionless state appears until de evaporation finish with a unwetting sequence. The sequence of convective patterns obtained here without heating, is similar to that obtained in Bénard-Marangoni convection. This work present the sequence of spatial bifurcations as a function of the layer depth. The transition between square to hexagonal pattern, known from non-evaporative experiments, is obtained here with a similar change in wavelength.

Introduction. – Pattern formation in different areas of knowledge had received great attention in the last decade [1, 2]. Interest in this kind of research arises from the general interest in nature understanding and also from requirements of industrial processes like painting, film drying or crystal growth, where pattern formation knowledge plays a fundamental role. Pattern formation during evaporation is a common phenomena that can be frequently observed in nature. Natural convection self-generated by the evaporation of a thin layer of water, normally left the brand of its individual convective cells in the bottom clay.

Since the first rigorous work devoted to study pattern formation in fluids [3] the existence of cellular structures was recognized be linked to surface tension and buoyancy. Experimental and theoretical studies where movements are generated mostly by interfacial forces [4, 5] have been increased in the last years [6, 7]. Generally convective movements originated in surface tension gradients are associated with the names Marangoni or Bénard-Marangoni convection (BM). In evaporative convection there are two main physical mechanisms of instability relating surface tension gradients, one with a change in the composition or concentration, so called *thermosolutal convection* and the other with the local dependence of surface tension with temperature or *thermocapillary convection*.

(*) e-mail address: hmancini@fisica.unav.es

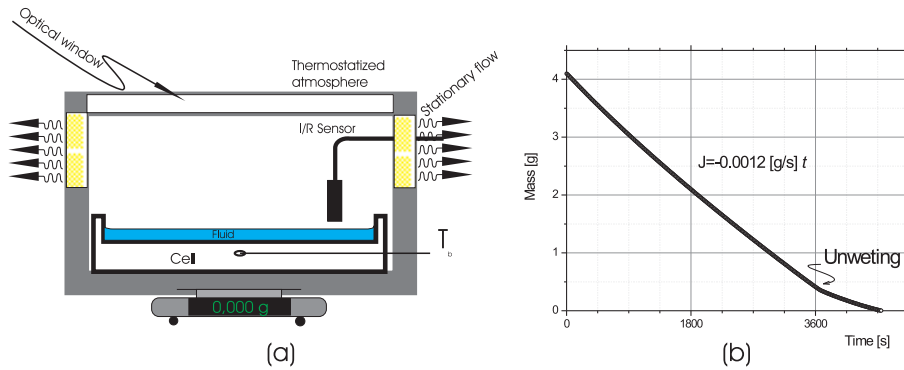


Fig. 1 – (a) Scheme of the experiment: a cylindrical cell is mounted in a closed environment where a very small flow refresh air and vapor pressure. (b) The pressure unbalance drive an almost linear evaporation rate until the drying process begins.

In the first one, experiments are normally performed using alcohols or other evaporative fluids like polymers in solution where the proportion between solute and solvent can be changed by evaporation [8, 9]. As an example, Zhang & Chao [10] presented an experimental work reporting the onset of patterns considering heating (or even cooling) and evaporation using this kind of fluids. They used a thin liquid layer of alcohol (between others liquids) heated from below and the convective structures have been observed by seeding the fluid with aluminum powder.

In pure thermocapillary convection, temperature is involved directly and movements are now related with local temperature dependence of surface tension. Hydrodynamics instabilities grows as in the Bénard original works, but in our knowledge there are not exist previous experimental results of pattern formation in evaporation of pure fluids. Recently Maillard et al. [11] presented a microscopic evidence of unusual patterns (micron sized objects like rings and hexagonal arrays) that they consider patterns of Bénard-Marangoni convection driven by surface tension gradients. Even if the work is not performed with an evaporative fluid, it certify that interest is arising from material science in the production and control of well-ordered arrays of this kind of cells at micron scale.

Regarding properties of evaporation there is a family of experimental and theoretical studies aiming to determine constants like the Sherwood number (the adimensional rate of evaporation) under different conditions, [12, 13] or the temperature profile near the evaporating surface [14, 15]. Normally, pattern formation is not an specific object of these works and must be said that the simultaneous measurement of all parameters involved is normally a complex task.

In all the experiments above mentioned, patterns are composed mostly by irregular cells. Normally aspect ratio is large (we call aspect ratio Γ , the proportion between the horizontal characteristic dimension and depth). In the former experiments, to our knowledge, no attempts has been made to compare evaporative experiments with theory in the frame of pattern formation. The present work is the first experiment devoted to check the convective pattern sequence appearing in an evaporation layer without heating and to compare it with non evaporative convection.

The experiment. – It is well known from thermodynamics that equilibrium in a fluid with its vapor phase is bidimensional. The equilibrium states are all on a line in the plane defined by pressure p , and temperature T . In a closed environment with a layer of volatile fluid, the fluid evaporates until the vapor phase reaches the vapor pressure corresponding to the fluid temperature. When the equilibrium pressure is reached evaporation stops. If a part of the atmosphere composed by air plus vapor is removed (i.e. blowing slightly), the fluid tends to evaporate continuously until recover its equilibrium value. If the volume of air is replaced at the same rate that the mixture of vapor plus air is removed, a constant evaporation rate can be reached. Under this condition evaporation follows until all the liquid layer disappear. This a common situation in nature when the wind removes the vapor phase in equilibrium with a fluid and makes to evaporate completely a volatile layer.

In the experiment here presented we reproduce this conditions introducing all the set-up in a closed box and evacuating a small part of the total volume of the inner box atmosphere. A scheme of the system can be seen in Fig. 1.a.

The fluid used was hexamethyldisiloxane ($C_6H_{18}OSi_2$) and it was choosed because it is a pure volatile fluid at atmospheric pressure (Prandtl number = 14.5). Properties of this and other silicon oils can be obtained from different handbooks [16, 17]. It was placed in a cylindrical container on an electronic analytical balance in order to measure in real time the mass evaporated (with a precision of 0.001 g). The atmosphere at the inner of the box, composed by the vapor pressure of the fluid plus air, was kept at a constant pressure by refilling with a laminar flow of new air at the same temperature and at the same rate of evacuation. This stationary state, slightly out of equilibrium, generates a constant rate of evaporation. The evaporation rate \mathbf{J} is defined by the rate at which the vapor pressure is removed from the gas phase and by the temperature of the fluid phase.

There is no external heating or cooling in this experiment. The latent heat is the responsible for convection. The pool is left to reach its own thermal equilibrium with the environment in a time that depends on its thermal conductivity. Thermal exchanges are restricted to different parts of the system at the inner of the box. The box with all the system is placed in a conditioned air room in order to keep constant also the external temperature. The latent heat extracted from the fluid is subsequently recovered from the surroundings of the layer. Two extreme conditions of conductivity had been used in the container of the fluid to check their influence. One was a good conductor aluminum cell and other with equal dimensions and geometry but constructed in a thermal isolator material. We do not found significative differences in the patterns obtained further the different recovery times.

In the experiment, patterns appears spontaneously if the evaporation rate and the fluid depth are adequate. To obtain ordered patterns the evaporation rate \mathbf{J} must be relatively low. In a typical sequence \mathbf{J} was controlled between $0.0010\text{ g/s} < \mathbf{J} < 0.0015\text{ g/s}$. Depth of the fluids are obtained from this value, the volume of the cylindrical container (Area = 80.12 cm^2), and the fluid density (0.760 g/cc). A typical evaporation rate obtained in the experiment can be seen in Fig 1.b. It is interesting to note that only when the drying process of the layer begins there is a sudden change in the evaporation rate.

Before the unwetting (or drying process) and without refilling the cell with new fluid, the depth of the layer changes linearly from a fixed and arbitrary initial value to zero, independently of what kind of patterns appear.

Pattern dynamics. – Patterns are observed by a usual shadowgraph techniques described in other former experiments of the authors [18]. The transient sequence of patterns shown in Fig.2, have been obtained when a linear change in depth with time is prepared in the experiment. We used an image processing system to captures images that then are processed

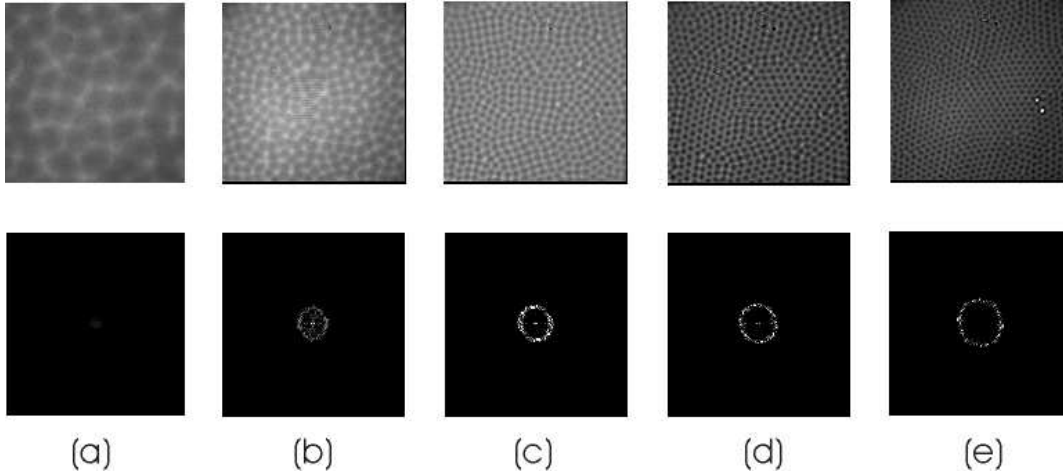


Fig. 2 – Sequence of patterns obtained as a function of decreasing depth and its FFT spectrum. (a) $d = 0.8 \text{ mm}$. (b) $d = 0.7 \text{ mm}$. (c) $d = 0.6 \text{ mm}$. (d) $d = 0.5 \text{ mm}$. (e) $d = 0.4 \text{ mm}$.

and stored together with the corresponding outputs of the data acquisition system. Images and data files of temperatures, depth and evaporation rate obtained at the same time are then used to obtain the results here presented. The error in time synchronism of all the system is negligible. To control the results, each experiment has been performed more than 20 times. It was verified that if the evaporated mass is refilled to the pool keeping depth constant, a really stationary pattern can be obtained. As shown in Fig. 1.b, the change in depth at a fixed evaporation rate fits an almost linear function. The second order coefficient (deviation from linearity) is obtained reproducibly and is two orders of magnitude lower than the linear coefficient.

The sequence begins when the cell is filled with a fixed and arbitrary initial depth of fluid (normally we used $d_0 = 2 \text{ mm}$). Considering the diameter of the cell it means an initial aspect ratio of $\Gamma \approx 50$. Initially, convective movements are in turbulent phase. Movements are mostly formed by thermals which born at the bottom of the cell and appear randomly distributed in space and time. When the layer depth goes under a certain value, typically $d = 0,8 \text{ mm}$, a pattern formed by a few irregular and large cells fills the pool (Fig. 2.a). Lowering the layer depth, the size of the cells is lower and consequently the number of cells increase (Fig. 2.b). The planform changes continuously with depth to a pattern composed by tetragonal cells (Fig 2.c).

If depth goes down to $d = 0.5 \text{ mm}$ approximately, suddenly the pattern composed by domains of tetragonal cells of Fig. 2.c changes to other of hexagonal cells like in the Fig.2.d, that exist until a critical depth d_c is reached. When the minimum depth is reached all the pattern disappear until that "drying process" begins. Drying means destruction of the layer and begins when a long wavelength instability appears giving place to other different stage in the experiment. The FFT sequence displayed in Fig. 2, show the existence of a well defined wavenumber but without a preferred direction in the phase plane.

Fig. 3.a display a typical data file of the mean wavelength against supercriticality in a run. We have defined here the supercriticality $\epsilon = \frac{d-d_c}{d_c}$ as the parameter distance from the critical depth d_c in order to compare with the results obtained in a non-evaporative convection with heating [6].

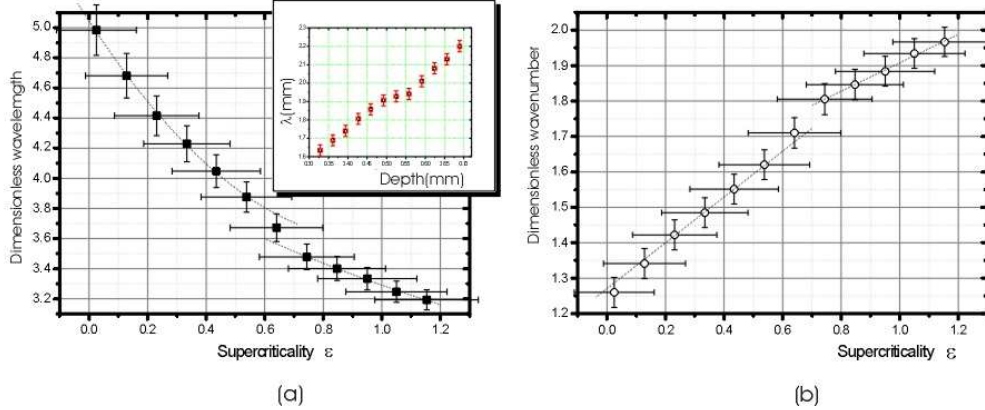


Fig. 3 – (a) Mean dimensionless wavelength as a function of the distance to the critical depth d_c . The inset show the dimensional wavelength as a function of the liquid depth. Note the existence of a transition zone corresponding to the square to hexagon transition. (b) Dimensional wavenumber as a function of the supercriticality. The fits are just guide for the eye.

Experiments on square to hexagon transition (*SHT*) has been only recently reported [19, 20]. This transition shows strong hysteresis effects. The wavelength at the transition of hexagons to squares (when ϵ is increased) is 10% lower than the wavelength when the supercriticality is diminished. In our experiment, such hysteresis effect can not be measured. We observe a "jump" in the dimensionless wavelength when the *SHT* take place (Fig 3.a). Note from the inset in the Fig 3.a, that the medium wavelength of the cellular pattern remains almost constant for depth between $0.49 \text{ mm} < d < 0.56 \text{ mm}$. This fact implies approximately a jump of 5% in the wavelength normalized by the depth of the fluid.

Within our optical test resolution, we determine almost the same critical depth $d_c = 0.3 \text{ mm}$, for all the evaporation rate studied. The dimensionless wavenumber $k_c = 1.25$ corresponding to the onset (Fig 3.b), is in disagreement with the predicted value for the linear theory [21, 22] which is $k_c = 1.97$. This disagreement can be related with the fact of the convective pattern at threshold not is stationary but have a characteristic life-time related with the evaporation rate \mathbf{J} and the horizontal diffusion time. A more advanced experimental setup, where the liquid depth remains almost constant during a horizontal diffusion time, is been implement in order to study the critical wavenumber at the onset. These results will be reported elsewhere.

Other outputs of the experiment are the local temperatures against time (or depth). To measure local temperatures at different depths, sub millimeter thermocouple are mounted laterally in a small hole on a plexiglass ring to avoid a pattern perturbation. Plexiglass is a thermal isolator having a similar conductivity to the silicon oil, so temperature recovering from the environment is obtained principally from the aluminum disk placed below. An infrared sensor (IR) is used to measure the temperature at the free surface. From the thermocouple putting inside the cell, we determine temperature dynamics. Two regimes can be identified: (a) when the fluid is in turbulent regimen, the temperature difference between fluid and atmosphere rise to a limit value between -0.8°C to -1.0°C and (b) when the stationary pattern stabilizes, this difference decrease to -0.4°C and remains almost constant to the unwetting process. Finally the temperature goes up to the initial equilibrium value.

Discussion. – In this experiment appear a typical sequence of ordered patterns similar to a Bénard-Marangoni convection heated from below. As the sequence appear here without any external heating, only very few of the previously existing models describing evaporation patterns are useful. The typical cellular patterns obtained can be observed and measured reproducibly. As during the evaporation the fluid layer depth goes down, the control parameter is consequently lower and the sequence obtained is inverted in order respect to normal BM convection.

The first effect produced by evaporation in our experiment is to create the vertical temperature gradient by latent heat. So we do not need any heating or cooling flow. The second one is to increase the thermal conductivity in the evaporating surface. It means to increase the cooling in the cold surface points and the heating in the hot one's. This in turn increases the effective Biot number in the models. It can be verified experimentally by observing that the system become strongly turbulent when the evaporating rate is increased too much. To have ordered patterns the flow of mass must be controlled.

Normally the theoretical models for this kind of experiments consider an externally imposed heating or cooling flow (from below or from above). Very recently appeared a theoretical work of Merkt & Bestehorn [23] where this sequence is obtained without external driving. They constructed two theoretical models, one is two layer (fluid and gas) approximation where they perform a linear stability analysis. The other is a one layer approximation with a large effective Biot number.

With the second one they found that thresholds obtained in non-evaporating oils with a fixed Prandtl number fluid ($Pr=10$) are significantly lowered with increasing the Biot number. The pattern morphology is reproduced and the sequence of bifurcations obtained in our experiment is then reproduced numerically (even if there are some differences in the numerical values). The high effective Biot number hypothesis is very acceptable for us and also is reinforced because we use an small air flow to carry slightly out of equilibrium the system. This must further increase the heat exchange, equivalent at to have a better heat conduction in the top surface (an even higher Biot number).

Conclusions. – In summary, we presented here the first experimental report of ordered spatial bifurcations produced only by evaporation and a time solved information of the relevant variables. The sequence of pattern described is the same as in non-evaporative convection for a control parameter increasing its value. The main features of the experiment can be explained by a recent theory [23]. We demonstrate that patterns exist in a well defined range of depths and also that the transition between squares to hexagons appear as clearly as in non-evaporative convection, with a change in the dimensionless wavenumber similar to the value reported for non evaporative convection. The tetragonal structure appears when convection is more important to the heat transport (higher depth) and this result confirm also that tetragonal cells seem to be more efficient than hexagonal in heat transport, as was assumed in [19].

* * *

Authors thanks to M. Bestehorn for share with us their theoretical results and for accept to exchange it with our experimental results before publication. Also we are indebted to Iker Zuriguel for his participation in the first stages of this experiment and Emmanuel Mancini for the cooperation in the construction of the experimental set-up and during the development of measurements. This work was partially supported by the European Community network ECC TRN HPRN-CT-2000-00158 and by MCyT project BFM2002-02011, Spain.

REFERENCES

- [1] CROSS M. C. and HOHENBERG P. C., *Rev. Mod. Phys.*, **65**(1993)851
- [2] RABINOVICH M., EZERSKY A. and WEIDMAN P., *The Dynamics of Patterns* (World Scientific, Singapore) 2000
- [3] BÉNARD H., *Rev. Gé. Sci. Pures Appl.* **11** (1900) 1261
- [4] BLOCK M., **178** (1956) 650
- [5] SCRIVEN L.E. and STERLING C.V., *Nature* **187** (1960) 186
- [6] COLINET P., LEGROS J.C. and VELARDE M.G., *Nonlinear Dynamics of Surface-Tension-Driven Instabilities* (Wiley, Berlin) 2001
- [7] NEPOMNYASHCHY A., VELARDE M. G. and COLINET P., *Interfacial Phenomena and Convection* (Chapman and Hall-CRC, EE UU) 2002
- [8] DE GENNES P-G., arXIV: cond-mat/0111167 (2001)
- [9] FANTON X. and CAZABAT A. M. , *Langmuir* **14** (1998) 2554
- [10] ZHANG N. and CHAO D. F., *Int. Comm. Heat Mass Transfer* **26** (1999) 1069
- [11] MAILLARD M., MOTTE L., NGO A. T. and PILENI M. P., *J. Phys. Chem. B* **104**,(2000) 11871
- [12] SPARROW E. M. and NUNEZ G. A., *Int. J. Heat and Mass Transfer* **31** (1988) 1345
- [13] SAYLOR J. R. , SMITH G. B. and FLACK K.A., *Phys. Fluids* **13** (2001) 428
- [14] FANG G. and WARD C. A., *Phys. Rev.E* **59** (1999) 417. FANG G. and WARD C. A., *Phys. Rev.E* **59** (1999) 429. FANG G. and WARD C. A., *Phys. Rev.E* **59** (1999) 441
- [15] BEDEAUX D. and KJELSTRUP S., *PhysicaA* **270**, (1999)413
- [16] *Polymer Data Handbook. J. E. Marx, Edit.* (Oxford Univ. Press New York) 1999
- [17] *NIST Chemistry WebBook* (<http://webbook.nist.gov>) 2003
- [18] ONDARÇUHU T., MILLAN-RODRIGUEZ J., MANCINI H. L., GARCIMARTÍN A. & PÉREZ GARCÍA C., *Phys. Rev. E* **48**(1994)1121
- [19] ECKERT K., BESTEHORN M. and THESS A., *J. Fluid Mech.* **356** (1998) 155.
- [20] VANHOOK S., J.SCHATZ M. F., SWIFT J.B., MCCORMICK, W. D. and SWINNEY H.L., *Phys. Rev. Lett.* **75** (1995) 4397.
- [21] PEREZ GARCIA C., ECHEBARRIA B., BESTEHORN M., *Phys. Rev. E* **57** (1998) 475.
- [22] SCHATZ M. F., VANHOOK S. J., MCCORMICK, W. D., SWIFT J.B. and SWINNEY H.L., *Phys. Fluids* **11** (1999) 2577.
- [23] MERKT D. and BESTEHORN M., *Physica* **D185** (2003)196